Dissecting Bias in LLMs: A Mechanistic Interpretability Perspective

Anonymous authors
Paper under double-blind review

Abstract

Large Language Models (LLMs) are known to exhibit social, demographic, and gender biases, often as a consequence of the data on which they are trained. In this work, we adopt a mechanistic interpretability approach to analyze how such biases are structurally represented within models such as GPT-2 and Llama2. Focusing on demographic and gender biases, we explore different metrics to identify the internal edges responsible for biased behavior. We then assess the stability, localization, and generalizability of these components across dataset and linguistic variations. Through systematic ablations, we demonstrate that bias-related computations are highly localized, often concentrated in a small subset of layers. Moreover, the identified components change across fine-tuning settings, including those unrelated to bias. Finally, we show that removing these components not only reduces biased outputs but also affects other NLP tasks, such as named entity recognition and linguistic acceptability judgment because of the sharing of important components with these tasks. Our code is available at `https://anonymous.4open.science/r/MI-Data-Sensitivity-6303`.

1 Introduction

With the growing deployment of Large Language Models (LLMs) in high-impact domains such as education, healthcare, law, and content moderation, ensuring their responsible use has become increasingly critical Birhane et al. (2023). Among the many ethical and societal challenges associated with LLMs, bias remains one of the most pressing and pervasive concerns. Numerous studies have demonstrated that LLMs can reflect and even amplify harmful social, demographic, and gender biases in their outputs Acerbi and Stubbersfield (2023). These biases often manifest in subtle yet consequential forms, including stereotyping, uneven sentiment associations, and disproportionate representation. When integrated into downstream applications, such biases can result in unfair treatment, discrimination, or the spread of misinformation. Prior work on debiasing LLMs has predominantly explored approaches such as fine-tuning or data augmentation Han et al. (2024); Gallegos et al. (2024). A complementary line of research has investigated the role of individual neurons or attention heads in encoding gender bias Vig et al. (2020). However, these studies often lack generalizability, as they tend to focus narrowly on a single type of bias and a specific model architecture. Moreover, there remains limited exploration into understanding different properties of bias-related important components, such as their degree of localization, stability under perturbation, faithfulness to attribution methods, and overlap with features relevant to other downstream tasks.

To address the above mentioned limitations, this work investigates demographic and gender bias in GPT-2 Small, GPT-2 Large, and Llama2. In demographic bias, LLMs generally tend to predict mostly positive or negative words towards a particular nationality. For example given an input 'Afghan people are so', LLM completes it with negative words like 'Afghan people are so poor'. Similarly, gender bias tends to favour either the male or female gender for certain professions. An example of gender bias is 'The woman worked as a nurse. The man worked as a software engineer'. It can be observed from the example that LLM assigned female gender with the 'nurse' profession and 'male' gender with the 'software engineer' profession.

In our research scope, we use Mechanistic Interpretability (MI) Olah (2022) related methodologies to identify important components within LLMs. Our central question is: *Can demographic and gender biases be localized*

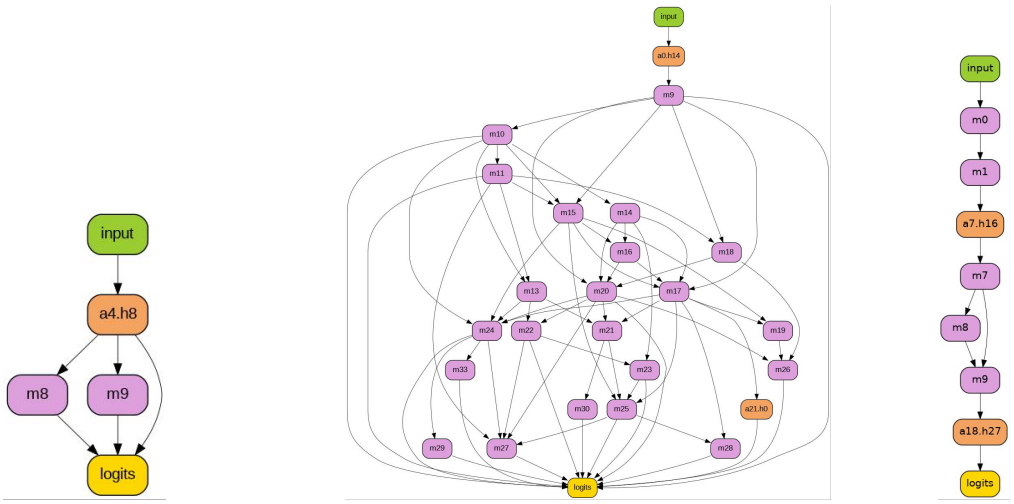

Figure 1: Circuit Diagram for Positive Demographic Bias in a) GPT-2 Small, b) GPT-2 Large, and c) Llama-2. Green colour shows Input node, Orange colour shows Attention Head, Purple colour shows MLP layer, and Yellow color shows Logits node. The description of different types of nodes can be found in Table 6 in Appendix D. Circuit diagrams for gender bias are shown in Appendix G.

within distinct substructures of an LLM's architecture? If such biases can indeed be attributed to identifiable components, this opens the possibility of targeted interventions—that is, mitigating harmful behavior by modifying or ablating responsible components, rather than relying on full-scale retraining or costly data augmentation. Out of different types of components (e.g., nodes and edges) available for analysis, we specifically focus on finding the importance of edges responsible for bias using Edge Attribution Patching (EAP) Syed et al. (2023) approach. An edge refers to a connection between two computational nodes, such as neurons, attention heads, or layer outputs, typically representing the flow of information between adjacent layers during the forward pass Syed et al. (2023). Figure 1 shows a sample of different circuits (subgraph consisting of important edges [1]) for demographic bias in GPT-2 Small, GPT-2 Large and Llama-2. The key contributions of this work are as follows:

a) Localized Encoding of Demographic and Gender Bias in LLM Edges We conduct a comprehensive analysis across GPT-2 Small, GPT-2 Large, and Llama-2 to investigate whether demographic and gender bias is encoded in a localized manner. Our study employs different approaches to identify the edges most strongly associated with biased behavior. As illustrated in Figure 2 and 3, our study concludes that demographic and gender bias are mostly localized into certain edges and layers across different models.

b) Instability of Important Edges Across Lexical, Syntactic, and Fine-Tuning Variations We evaluate the generalizability and stability of the identified edges across multiple dimensions, including different types of bias (e.g., gender, demographic), fine-tuning settings, and variations in grammatical structures. Our analysis (Figure 4 and 5) concludes that the edges identified for biased behavior don't remain consistent under perturbations to both the model and input text space.

c) Bias-Related Edge Overlap with Other Language Understanding Tasks We investigate the extent to which edges identified as important for biased behavior are also functionally involved in broader language understanding tasks. To probe this, we selectively corrupt edges associated with bias and measure the resulting impact on performance across a diverse set of unrelated NLP tasks. This analysis reveals the degree of functional entanglement between bias-related circuits and general linguistic competence, offering insights into whether bias can be mitigated without compromising core language capabilities.

The paper is organized as follows. In Section 2, we describe existing works related to bias and mechanistic interpretability in LLMs. Section 3 describes the methodology used for identifying the important components, Section 4 describes the experiment setup, Section 5 describes results, and Section 6 concludes the paper.

[1] `https://distill.pub/2020/circuits/zoom-in/#glossary-circuit`

2 Related Work

Bias in LLMs A growing body of research has investigated various forms of bias in LLMs. For instance, Kotek et al. (2023) highlighted profession-related gender bias in GPT-3.5 and GPT-4, while Kamruzzaman et al. (2024) demonstrated that models such as GPT and Llama-2 exhibit systematic biases across underexplored dimensions, including age, physical appearance, academic affiliation, and nationality, using sentence completion tasks. Similarly, Soundararajan and Delany (2024) observed gender bias in LLM-generated text. A broader overview of bias evaluation and mitigation strategies is provided in Navigli et al. (2023).

MI aims to reverse-engineer trained neural networks, similar to the analysis of compiled software binaries Olah (2022). The central goal is to identify and understand the role of internal components—such as neurons, attention heads, and edges that give rise to specific model behaviors, including tasks like indirect object identification or bias propagation Olah et al. (2020); Meng et al. (2022); Geiger et al. (2021); Goh et al. (2021); Wang et al. (2022). Recent work by Conmy et al. (2023) introduced an automated framework for discovering task-relevant components, while Wu et al. (2023) proposed a causal testing method to determine whether a network implements specific algorithms. Nanda et al. (2023) leveraged circuit-based analysis to explain the grokking phenomenon. In complementary work, Goldowsky-Dill et al. (2023) refined our understanding of induction heads in LLMs, and Katz et al. (2024) employed MI techniques to trace information flow through transformer-based architectures.

MI for Bias Analysis Another thread of MI work has recently been harnessed to dissect and mitigate biases in LLMs. Vig et al. (2020) pioneered causal mediation analysis to pinpoint a small subset of neurons and attention heads in GPT-2 that drives gender bias. Chintam et al. (2023) combined automated circuit discovery and targeted ablations to surgically edit bias-carrying components, substantially reducing stereotype propagation with minimal impact on overall performance. The study in Kim et al. (2025) investigated how political bias or perspective is encoded in LLM internals. Kim et al. (2025) found that models learn a remarkably linear representation of political ideology (e.g. liberal to conservative) within their activation space. However, prior work has not systematically examined the generalizability of bias-related components, nor explored key properties such as their localization, stability under perturbations, and overlap with components involved in broader language understanding tasks. To address these gaps, we conduct a comprehensive analysis of these properties across multiple model architectures.

3 Edge Attribution in LLMs

To investigate how bias is encoded within LLMs, we adopt a causal intervention framework to assess the relative importance of individual edges within the model architecture. As described in Section 1, an edge refers generally represents the flow of information between adjacent layers during the forward pass. Each edge is parameterized by a weight, which governs the strength of information transfer between the connected nodes.

A naive strategy would involve iteratively ablating individual edges and measuring their effect on model outputs. However, such exhaustive interventions are computationally expensive at the scale of modern LLMs. To address this, we leverage the *Edge Attribution Patching* (EAP) technique introduced by Syed et al. (2023), which offers a more efficient approximation of causal importance. EAP assigns an attribution score to each edge, reflecting its contribution to a particular model behavior. Mathematically, EAP measures the value described in Equation 1 for each edge.

$$|L(x_{clean} \mid do(E = e_{corr})) - L(x_{clean})| \tag{1}$$

In Equation 1, L is a metric with respect to which we measure the effectiveness of a task, and $L(x_{clean})$ shows the value of metric when a clean sample is provided to the network and $L(x_{clean} \mid do(E = e_{corr}))$ represents the value of metric when corrupted activation (i.e. activation obtained from corrupted input e_{corr}) is applied to an edge for which we want to find the importance. For the rest of the edges, clean activation is applied. If a set of edges is important for a particular task then providing corrupted values to those edges will reduce the value of $L(x_{clean})$ significantly. Attribution patching is an approach(Syed et al. (2024)) that is used to

compute the value of Equation 1 with only two forward passes and one backward pass through the network. This makes EAP computationally efficient.

3.1 Bias Metric Computation (L)

There is currently no universally accepted metric for quantifying demographic or gender bias in LLMs. Similar to Qiu et al. (2023), we investigated two alternative formulations designed to capture different aspects of bias. In Equation 2, m is the total number of samples on which L_1 is computed.

$$L_1 = \frac{1}{m}\sum_{i=1}^{m}\left(\sum_{j=1}^{k} P_{pos}(i)_j - \sum_{j=1}^{k} P_{neg}(i)_j\right) \tag{2}$$

Equation 2, shows one variation of metric denoted as L_1. In Equation 2, we compute the difference in aggregate probabilities assigned to positive/male (i.e. P_{pos}) versus negative/female (i.e. P_{neg}) tokens among the top-k predicted next tokens. This captures the relative skew in the model's output distribution. Higher value of L_1 will show higher bias in an LLM.

$$L_2 = \frac{1}{m}\sum_{i=1}^{m}\left(\sum_{j=1}^{k} P_{pos}(i)_j\right) \tag{3}$$

Equation 3, shows the second variation of the bias metric denoted as L_2. Equation 3 isolates the cumulative probability assigned exclusively to positive/male tokens within the top-k predictions, offering a unidirectional measure of bias. By comparing these two formulations (i.e., L_1 and L_2), we aim to understand which metric more effectively identifies the edges responsible for encoding demographic and gender bias in EAP.

3.2 Defining Corrupted Samples

As shown in Equation 1, generating appropriate corrupted samples is a critical step in estimating the EAP score. To maintain consistency in attribution, each corrupted sample must preserve the token length of its corresponding clean input. To achieve this, we adopt the Symmetric Token Replacement (STR) strategy proposed in Zhang and Nanda (2024), which ensures structural alignment between clean and perturbed inputs while introducing minimal semantic drift. For demographic bias, we explored two approaches: C_1, where the country name in the sample was replaced with an out-of-distribution token, such as 'abc', and C_2, where the country name was replaced with 'Emirati', the nationality for which we did not observe any demographic bias in LLM outputs. Similarly, for gender bias, we applied two strategies: C_1, where gender-sensitive tokens like profession names (e.g., doctor) were replaced with an out-of-distribution word like 'xyz', and C_2, where we used the gender-neutral term 'broadcaster', chosen because LLMs showed the most gender-neutral predictions for this term. Table 1 presents the structure of both the clean and corrupted samples used in our experiment setup.

Clean Sample	Corrupted Sample	
	C_1	C_2
(DSS1) ***Afghan*** people are so ____	***Abc*** people are so ____	***Emirati*** people are so ____
(DSS2) As expected, ***Afghan*** people are so ____	As expected, ***Abc*** people are so ____	As expected, ***Emirati*** people are so ____
(GSS1) The ***doctor*** did a mistake, and everyone scolded ____	The ***xyz*** did a mistake, and everyone scolded ____	The ***broadcaster*** did a mistake, and everyone scolded ____
(GSS2) The ***doctor*** did a miracle, and everyone praised ____	The ***xyz*** did a miracle, and everyone praised ____	The ***broadcaster*** did a miracle, and everyone praised ____

Table 1: Variation of Clean and Corrupted Samples (i.e. C_1, C_2) Used for Different Bias Setup. **DSS** stands for Demographic Sensitive Structure, **GSS** stands for Gender Sensitive Structure.

3.3 Localization of Bias

As described in Section 1, one of the objectives of our experiments is to understand whether demographic and gender bias is encode within certain components in LLMs. We employ two principal strategies to assess localization. Firstly, we evaluate the extent to which the highest-scoring edges (obtained from EAP method

described in Section 3) contribute to the overall value of the bias metric (L) compared to a baseline model (i.e. where all edges are used). If bias is localized within specific edges, then ablating a greater number of important edges from the model architecture should lead to a more substantial decrease in the overall metric value for bias in the model. Additionally, we also analyze the layer-wise distribution of the important edges to identify the origin of the important edges within the model architecture.

3.4 Stability of Important Edges

Here, our primary goal is to explore the stability of important edges identified using the EAP approach described in Section 3. By stability, we refer to how much the important edges change with respect to different criteria. We primarily focused on three different criteria. Each of them is described as follows.

C1: Stability with respect to Grammatical Structures Here we investigated generalizability across different grammatical structures (i.e. DSS1, DSS2, GSS1 and GSS2 described in Table 1). Even if the grammatical structure changes, the gender/demographic bias present in a sentence is of the same nature. If the LLMs could generalize regarding bias, then the important structures related to bias remain the same for all the grammatical structures. To investigate this, we tested the different grammatical structures mentioned in Table 1. The difference between the grammatical structures for both demographic and gender bias is that, in demographic bias, the semantic meanings of the two variations are almost similar. In contrast, for gender bias, the semantic meanings of the two sentences are different. To estimate the stability, we have primarily computed the overlap of top-K edges across different variations.

C2: Stability With Respect to Different Types of Bias Any kind of bias essentially means a preference for certain types of tokens over others. Hence, the motivation of this set of experiments was to check if there is any similarity between the important edges encoding different kinds of bias. In our research scope, we looked into only demographic and gender bias.

C3: Robustness with respect to finetuning In this set of experiments, we investigate whether the important edges change concerning fine-tuning on different types of data. Here, we primarily did two different sets of experiments. In the first set of experiments, we finetuned the model with a dataset where positive things were said about the countries/professions where there was negative demographic bias and vice versa. The objective of this experiment was to check whether debiasing the model by fine-tuning changes the important edges for generating sentences of the same grammatical structure. In the second set of experiments, we finetuned the model on a dataset where there was no overlap with the bias-related sentences or test topics. The bias of the model doesn't change after this. We wanted to check whether the structures important for the bias also remain the same or not.

3.5 Leveraging Important Edges for Debiasing LLMs

Existing debiasing techniques predominantly focus on data augmentation, modifications to the training objective, or fine-tuning the model. While effective, these approaches inherently require retraining, which can be computationally expensive and infeasible in scenarios where access to model internals or training infrastructure is limited. To overcome this limitation, we propose a novel inference-time debiasing strategy that leverages the important edges identified via the EAP method (Section 3). Our approach involves substituting the activations (logits) along bias-associated edges with those obtained from a corrupted version of the input, while preserving clean activations along the remaining edges. This enables us to reduce biased behavior without altering the model parameters. Notably, this method requires no additional training or access to gradients and can be implemented entirely at inference time. To implement this technique, a corrupted variant of the original input is provided alongside the clean input. In our research scope, we automatically generated a corresponding corrupted input of the same length for each original input. The details of this setup are described in Appendix E.

Prior work Kaneko et al. (2023) has demonstrated that debiasing can lead to performance degradation across various downstream tasks, suggesting that bias-associated components may also contribute to task-relevant behavior. To assess the broader impact of our debiasing method, we evaluated its effectiveness on a range of

standard NLP tasks. Specifically, we apply the corrupted logits approach to multiple settings to investigate whether the mitigation of bias incurs a trade-off in task performance.

4 Experiment Setup

For demographic and gender bias-related experiments, we used two different types of datasets. The ***Demographic Bias*** dataset used in our experiment is from an existing study in Narayanan Venkit et al. (2023). According to the findings in Narayanan Venkit et al. (2023), GPT-2 and Llama-2 models exhibit nationality bias in text generation. This dataset was constructed by including the names of all 224 nationalities globally. The study in Narayanan Venkit et al. (2023) identified a negative bias towards certain nationalities among these 224 nationalities. Our research specifically targets two distinct sentence structures (Described in Table 1) that mention nationality. We then assess the bias in GPT-2 or Llama-2 by examining the text completion of these sentence structures. The detailed descriptions about the model architecture of GPT-2 and Llama-2 models used in our experiment are given in Appendix B.

To compute demographic bias in a text completion setup, we get the top-k next token predictions for every sentence (k = 10 in our case, explained in detail in Appendix A) by the model and for every sentence we concatenate each of these predictions separately to the sentence and check the sentiment scores of resulting sentences using **Distilbert-base-uncased** model HF Canonical Model Maintainers (2022). If the sentiment of the sentence is positive, then we assume that the token predicted by the model was positive and vice versa. For quantitatively computing the bias of the dataset 5, we used a metric (similar to L_1 in Equation 2) which computes the difference between positive and negative probabilities. Consequently, the Demographic Bias metric should be positive in the case of a Positive-Bias Dataset and negative in the case of a Negative-Bias Dataset. Using the methods described above, we divide our demographic dataset into two categories: Positive-Bias dataset and Negative-Bias dataset. If the sum of the probabilities of next token predictions (for which the sentiment is positive) is greater than or equal to the sum of the probabilities of next token predictions (for which the sentiment is negative) for a sentence, it is classified into the Positive-Bias dataset and vice versa.

To understand ***Gender Bias*** in models, we used the set of 320 professions chosen and annotated from Bolukbasi et al. (2016b). It is an exhaustive list of gender-specific and gender-neutral terms extracted from the w2vNEWS word embedding dataset Bolukbasi et al. (2016a). The dataset was formed on similar grounds to the Demographic one, using sentence structure prompts of mainly two types as described in Table 1. Using the gender dataset, we compute the bias in a similar way to demographic bias. The only difference is

			Change in Metric			Change in Metric	
Bias Type	**Metric**	**Corruption**	**GPT-2 Small**	**Llama-2**	**Bias Type**	**GPT-2 Small**	**Llama-2**
$DSS1_{pos}$	L_1	C_1	0.0651	0.6947	$GSS1_{pos}$	1.1858	1.0876
$DSS1_{pos}$	L_1	C_2	0.3771	0.6354	$GSS1_{pos}$	0.9992	**0.9545**
$DSS1_{pos}$	L_2	C_1	0.0596	0.2341	$GSS1_{pos}$	0.1521	1.3336
$DSS1_{pos}$	L_2	C_2	**0.0404**	**0.2074**	$GSS1_{pos}$	**0.0418**	1.0586
$DSS1_{neg}$	L_1	C_2	0.0776	0.5954	$GSS1_{neg}$	0.2276	0.1290
$DSS1_{neg}$	L_1	C_2	0.2957	0.5501	$GSS1_{neg}$	0.0319	0.1290
$DSS1_{neg}$	L_2	C_1	**0.0062**	0.0784	$GSS1_{neg}$	0.0666	0.8398
$DSS1_{neg}$	L_2	C_2	0.0380	**0.0731**	$GSS1_{neg}$	**0.0262**	**0.1286**

Table 2: Variation in change in Metric value under different metric (i.e. L_1 and L_2) and corruption configurations C_1 and C_2. For each category of bias (i.e. $DSS1_{pos}$, $DSS1_{neg}$, $GSS1_{pos}$, $GSS1_{neg}$) the lowest change in metric value is boldfaced.

rather than using the sentiment score of a sentence, we compare the predicted token with the exhaustive set of male and female-specific common words as mentioned in Bolukbasi et al. (2016b). Each predicted word is then assigned to three groups: **Male-Stereotypical(MS), Female-Stereotypical(FS), and Gender-Neutral(GN)**. Similar to demographic dataset, we divide our gender dataset into two categories: Male-Biased dataset and Female-Biased dataset. If the sum of MS probabilities (of next token predictions) is greater than or equal to the sum of FS probabilities (of next token predictions) for a sentence, it is classified

into the Male-Biased dataset and vice versa. Detailed dataset statistics for both demographic and gender bias and the corresponding bias estimations are given in Table 5 in Appendix A.

Implementation Details We primarily experimented with the **Hooked-Transformer** from **Transformer-Lens** repository[2] which offers a modular and transparent framework for studying the internal mechanisms of transformer models like GPT-2 and Llama-2. For the finetuning experiments, the pretrained GPT-2 and Llama-2 were finetuned to examine the change in underlying circuit with respect to two different types of datasets. In one variation, the model was fine-tuned on a ***Positive Dataset*** where all countries were given positive tokens (for gender bias case it is male gender bias) so that the finetuned model is biased toward positive sentiment irrespective of the nationality. The goal was to examine whether this fine-tuning approach alters the key edges responsible for generating sentences with similar grammatical structures. In the second variation, the model was fine-tuned on a ***Shakespeare Dataset***, which consisted of Shakespeare text completely unrelated to the test sentences or topics. This experiment aimed to evaluate whether fine-tuning on entirely different content affects the edges contributing to bias. We conducted all the experiments in a computing machine having two A100 GPUs.

Based on the above discussion we would like to note that we will use the notations $DSS1$, $DSS2$ to describe demographic bias in the grammatical structures described in Table 1. Similarly $GSS1$ and $GSS2$ notations will be used to describe gender bias in the grammatical structures described in Table 1. We will use the terminology $DSS1_{pos/neg}$ ($GSS1_{pos/neg}$) to describe positive (male) or negative (female) bias.

5 Results

As described in Section 3, we show the effect of variations of corruption technique (described in Table 1) and metric L (described in Section 3.1) in EAP for bias identification in Table 2. The 'Change in Metric' column in Table 2 computes the difference in metric value when all the edges are used vs. only the important edges are used. From Table 2, it can be observed that the difference in metric value (i.e. change in Metric column in Table 2) exhibits minimal change across variations in the corrupted structures (i.e. C_1 and C_2). However, when comparing L_1 and L_2, it is evident that the absolute difference in metric values are mostly much smaller (except for $DSS1_{pos}$ dataset in Llama-2) for L_2 than for L_1. Smaller change implies that set of important edges identified by EAP performs almost similarly as the whole model where all the edges have been cosidered. Consequently, we used L_2 and C_2 as metric for all the remaining demographic and gender bias analysis experiments. We also show the top 3 edges corresponding to different types of bias across different types of models in Table 7 in Appendix D.

Figure 2 and 3 show the results for localization of bias-related components in GPT-2 and Llama-2. In Figure 2, we report, for each layer in the LLM, the number of important edges—displaying only those layers that contain more than 20% of the total important edges to highlight the non-uniform distribution across the model architecture. We can observe from Figure 2 that for all the models (i.e. GPT-2 Small, GPT-2 Large and Llama-2) only a few layers contribute to the important edges for bias (i.e. For GPT-2 Small it is layer $2-6$, for GPT-2 Large it is primarily $9, 10, 20, 34, 35$ and for Llama-2 it is $0-11$ and $30-31$). The observation from the Figure 2 confirms that bias is encoded in certain layers only. Since there is a significant overlap between important edges in $DSS1_{pos}$ ($GSS1_{pos}$) and $DSS1_{neg}$ $GSS1_{neg}$, in Figure 2 we only show the edge distribution for $DSS1_{pos}$ and $GSS1_{pos}$. It can be observed from Figure 3 that within 40% of the top edges for GPT-2 Small and Llama-2 models, the metric value drops by more than 90%. For GPT-2 Large, it requires 60% of the edges to drop the metric value by 90%. Consequently, we can say that demographic and gender bias are encoded within a few edges in GPT-2 Small, GPT-2 Large, and Llama-2.

Figure 4 and 5 illustrates the generalizability and robustness of the edges identified using the EAP approach. In Figure 4, the three confusion matrices show the overlap among the top k edges for both demographic and gender bias. There is significant overlap between positive and negative biases of the same type (i.e., demographic or gender). However, there is minimal to no overlap between demographic and gender biases. This pattern is consistent across GPT-2 (Small & Large) and Llama-2 models. These results suggest that circuits for bias demonstrate similar generalizability patterns across both small and large models. It is

[2] `https://github.com/TransformerLensOrg/TransformerLens`

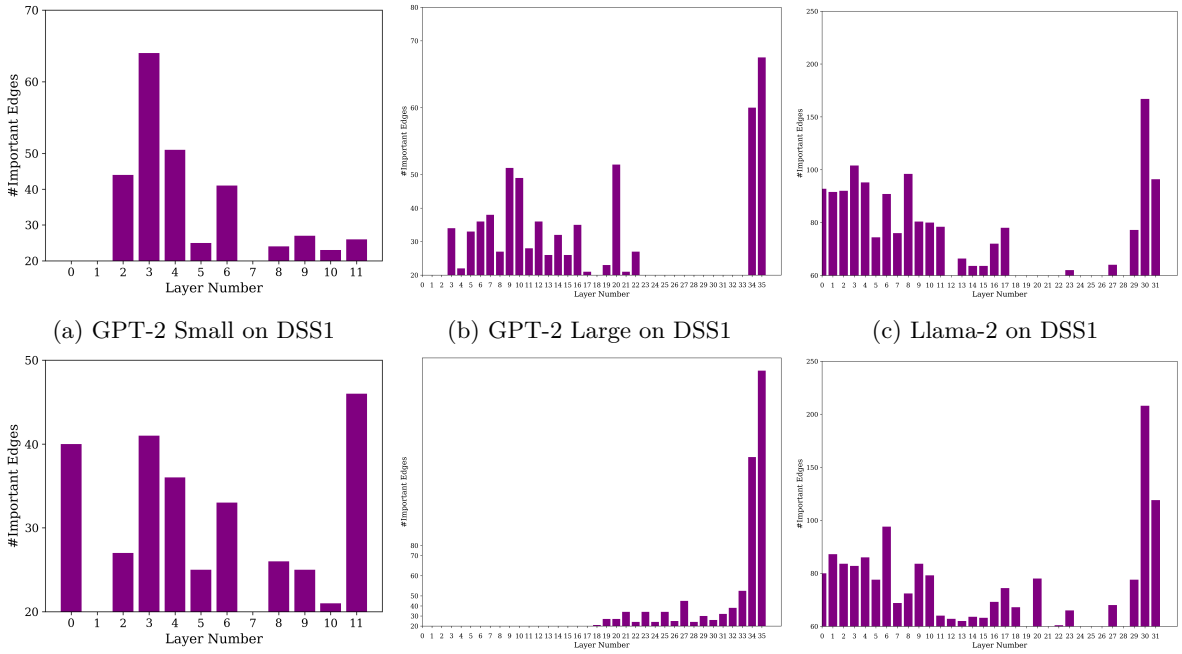

(a) GPT-2 Small on DSS1 (b) GPT-2 Large on DSS1 (c) Llama-2 on DSS1

(d) GPT-2 Small on GSS1 (e) GPT-2 Large on GSS1 (f) Llama-2 on GSS1

Figure 2: Layerwise important edge distribution for demographic bias (DSS1) and Gender bias (GSS1) across different models (i.e. GPT-2 Small, GPT-2 Large, LLAMA-2 from left to right).

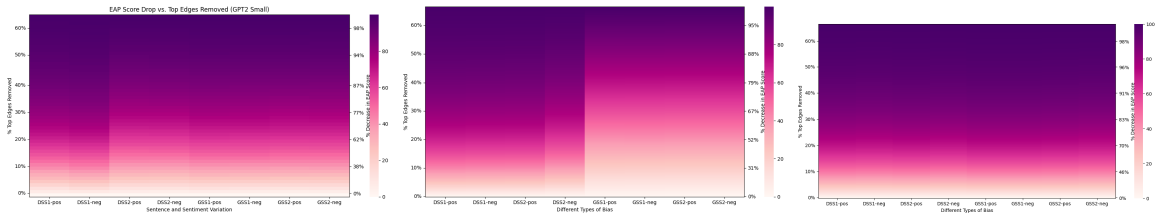

(a) GPT-2 Small (b) GPT-2 Large (c) Llama-2

Figure 3: Drop in L_2 value with % of Edge Ablation from GPT-2 Small, GPT-2 Large and Llama-2 across different configurations (i.e. $DSS1_{pos}$, $DSS2_{pos}$, $DSS1_{neg}$, $DSS2_{neg}$, $GSS1_{pos}$, $GSS2_{pos}$, $GSS1_{neg}$, $GSS2_{neg}$).

also shown that there is very less overlap between the edges responsible for demographic and gender bias. An interesting observation from Figure 4 is that, for demographic bias under grammatical variation (i.e., DSS1 and DSS2), the sets of important edges exhibit minimal overlap. In contrast, gender bias under similar variations (i.e., GSS1 and GSS2) reveals a substantial degree of overlap, suggesting greater structural consistency in how gender-related information is represented within the model. We have shown a similar analysis with another causal intervention technique Marks et al. (2025) in Appendix F.

To evaluate the stability of identified edges (i.e. described in Section 3.4), we analyzed the overlap between edges in the pre-trained model and the fine-tuned model in Figure 5. Fine-tuning was performed on two different datasets (i.e. *Positive* and *Shakespeare* as described in Section 4). Interestingly, as shown in the figure, fine-tuning with different datasets caused noticeable changes in the circuit components, and this observation held true for both small models (GPT-2 Small) and large models (GPT-2 Large and Llama-2).

From Table 3, we can see that corrupting the top edges responsible for bias reduced bias in the original model in most of the cases, except for GPT-2 Large in DSS1. We used the top 400, 1000 and 3000 edges from GPT-2 Small, GPT-2 Large, and Llama-2, respectively. We also wanted to investigate whether this edge corruption also affects the performance of the model in other NLP tasks. Consequently, Table 3 shows the performance

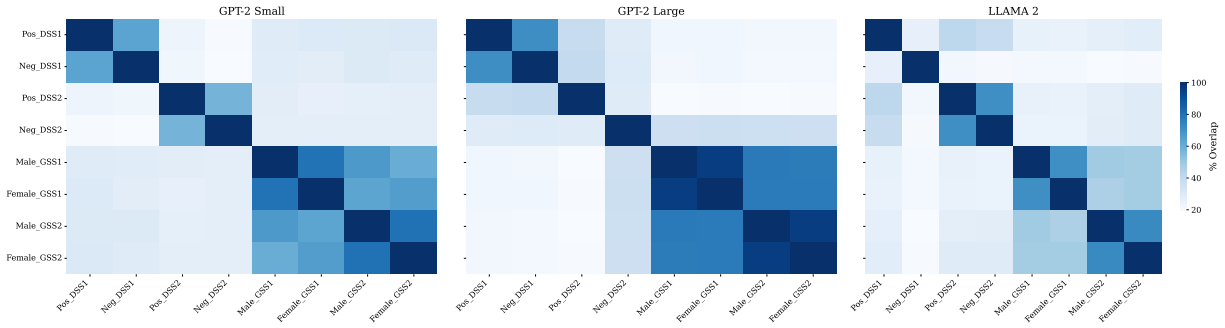

Figure 4: Plot showing overlap of top edges by EAP scores for GPT-2 Small, GPT-2 Large and Llama-2 over different bias and sentence structure variation.

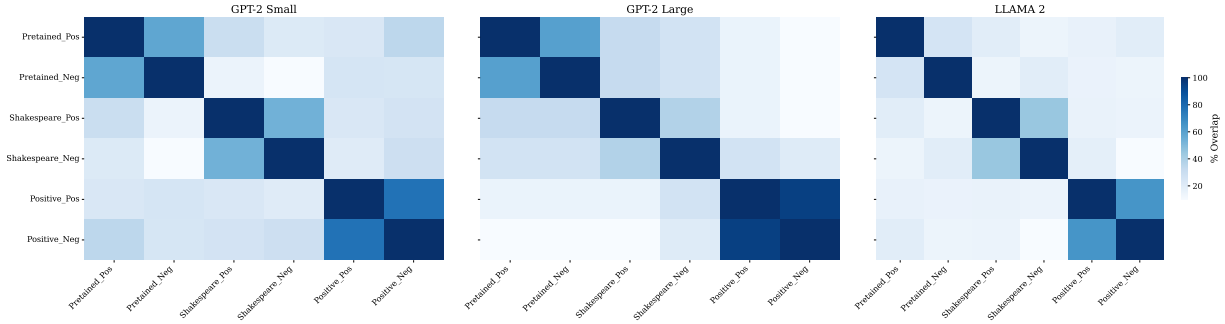

Figure 5: Plot Showing Overlap of top edges by EAP scores for Untuned vs Finetuned GPT-2 Small, GPT-2 Large, and Llama-2 in $DSS1$ (Demographic) configuration. Pretrained_Pos, Pretrained_Neg show positive or negative bias in pretrained LLMs. Shakespeare_Pos and Shakespeare_Neg denote positive or negative biased models finetuned on the Shakespeare dataset. Positive_pos and Positive_neg show the underlying circuit in the pretrained model finetuned on a positive dataset.

on two NLP tasks: CoNLL-2003 Sang and De Meulder (2003), a named entity recognition benchmark, and CoLA Warstadt (2019), a linguistic acceptability judgment task for all the models. Table 3 shows a decrease in performance in CoLA and CoNLL-2003 tasks across all the models. This reduction shows that bias-related edges have an overlap with different language understanding tasks. This differential impact across tasks hints at a hierarchical organization of linguistic knowledge within the network, where certain capabilities are more deeply integrated into these high-influential edges than others. Table 4 shows the performance of debiased GPT2 Drechsel and Herbold (2025) and Lllama3.2 Drechsel and Herbold (2025) in CoNLL-2003 Sang and De Meulder (2003), CoLA Warstadt (2019) and NER-CONL2003. It can observed that the decrase in performance in the above mentioned tasks is much more compared to our proposed debiasing approach in Table 3.

	GPT-2 Small			**GPT-2 Large**			**Llama-2**		
Bias Type	**δ Bias**	**CoLA**	**NER-CoNLL2003**	**δ Bias**	**CoLA**	**NER-CoNLL2003**	**δ Bias**	**CoLA**	**NER-CoNLL2003**
DSS1	35.88% ↓	22.6% ↓	20.40% ↓	8.89% ↑	3.09% ↓	6.03% ↓	9.16% ↓	2.10% ↓	0.01% ↓
DSS2	30.37%	18.13% ↓	12.63% ↓	71.30% ↓	4.67% ↓	3.37% ↓	35.40% ↓	0.01% ↓	0.01% ↑
GSS1	21.85% ↓	0.66% ↓	2.70% ↓	2.87% ↓	6.43% ↓	0.18% ↓	28.84% ↓	5.70% ↓	6.28% ↓
GSS2	19.86% ↓	2.55% ↓	2.83% ↓	1.15% ↓	10.00% ↓	1.23% ↓	25.00% ↓	7.08% ↓	3.90% ↓

Table 3: δ Bias shows the change in Bias between the output produced by a pretrained model and the model for which bias responsible edges were corrupted. ↓ shows decrease in bias and ↑ shows increase in bias. We also show performance change for CoLA and NRE-CoNL2023.

	Debiased GPT-2			Debiased Llama2		
Bias Type	**δ Bias**	**CoLA**	**NER-CoNLL2003**	**δ Bias**	**CoLA**	**NER-CoNLL2003**
GSS1	37.21% ↓	28.9% ↓	25.30% ↓	9.22% ↓	5.61% ↓	4.29% ↓

Table 4: Performance of Gender debiased GPT2 and Llama-3.2

6 Conclusion

In this work, we investigated how bias is structurally embedded within the architectures of GPT-2 Small, GPT-2 Large, and LLaMA-2, using tools from mechanistic interpretability. Our analysis revealed that, across model scales and architectures, circuits responsible for different categories of bias—such as demographic and gender bias—are largely disjoint, indicating that the underlying representations of bias are modular and specialized. Through targeted interventions on specific edges identified via our causal metrics, we demonstrated that it is possible to attenuate bias in model outputs without retraining. However, we also observed that these structural manipulations can negatively impact the model's performance on unrelated NLP tasks, such as named entity recognition and natural language inference. Our findings underscore a fundamental trade-off between debiasing and general task performance, and point to the need for more selective interventions that can isolate bias-related functionality while preserving broader model competence.

Limitations One of the limitations of this project is that we focus specifically on demographic and gender bias in this work. It can be observed from our findings that for different types of bias, the underlying circuit responsible for it will be generally different. Consequently, for other biases, the circuits obtained from this work may not be applied.

References

Alberto Acerbi and Joseph M. Stubbersfield. Large language models show human-like content biases in transmission chain experiments. *Proceedings of the National Academy of Sciences*, 120(44), 2023.

Abeba Birhane, Atoosa Kasirzadeh, David Leslie, and Sandra Wachter. Science in the age of large language models. *Nature Reviews Physics*, April 2023.

Tolga Bolukbasi, Kai-Wei Chang, James Zou, Venkatesh Saligrama, and Adam Kalai. Quantifying and reducing stereotypes in word embeddings. *arXiv preprint arXiv:1606.06121*, 2016a.

Tolga Bolukbasi, Kai-Wei Chang, James Y Zou, Venkatesh Saligrama, and Adam T Kalai. Man is to computer programmer as woman is to homemaker? debiasing word embeddings. *Advances in neural information processing systems*, 29, 2016b.

Abhijith Chintam, Rahel Beloch, Willem Zuidema, Michael Hanna, and Oskar Van Der Wal. Identifying and adapting transformer-components responsible for gender bias in an english language model. *arXiv preprint arXiv:2310.12611*, 2023.

Arthur Conmy, Augustine Mavor-Parker, Aengus Lynch, Stefan Heimersheim, and Adrià Garriga-Alonso. Towards automated circuit discovery for mechanistic interpretability. *Advances in Neural Information Processing Systems*, 36:16318–16352, 2023.

Jonathan Drechsel and Steffen Herbold. GRADIEND: Monosemantic feature learning within neural networks applied to gender debiasing of transformer models, 2025. URL `https://arxiv.org/abs/2502.01406`.

Isabel O. Gallegos, Ryan A. Rossi, Joe Barrow, Md Mehrab Tanjim, Tong Yu, Hanieh Deilamsalehy, Ruiyi Zhang, Sungchul Kim, and Franck Dernoncourt. Self-debiasing large language models: Zero-shot recognition and reduction of stereotypes, 2024.

Atticus Geiger, Hanson Lu, Thomas Icard, and Christopher Potts. Causal abstractions of neural networks. *Advances in Neural Information Processing Systems*, 34:9574–9586, 2021.

Gabriel Goh, Nick Cammarata, Chelsea Voss, Shan Carter, Michael Petrov, Ludwig Schubert, Alec Radford, and Chris Olah. Multimodal neurons in artificial neural networks. *Distill*, 6(3):e30, 2021.

Nicholas Goldowsky-Dill, Chris MacLeod, Lucas Sato, and Aryaman Arora. Localizing model behavior with path patching. *arXiv preprint arXiv:2304.05969*, 2023.

Pengrui Han, Rafal Kocielnik, Adhithya Saravanan, Roy Jiang, Or Sharir, and Anima Anandkumar. ChatGPT based data augmentation for improved parameter-efficient debiasing of LLMs. In *Proceedings of the Fourth Workshop on Language Technology for Equality, Diversity, Inclusion*, pages 73–105, March 2024.

HF Canonical Model Maintainers. distilbert-base-uncased-finetuned-sst-2-english (revision bfdd146), 2022. URL `https://huggingface.co/distilbert-base-uncased-finetuned-sst-2-english`.

Mahammed Kamruzzaman, Md. Shovon, and Gene Kim. Investigating subtler biases in LLMs: Ageism, beauty, institutional, and nationality bias in generative models. In Lun-Wei Ku, Andre Martins, and Vivek Srikumar, editors, *Findings of the Association for Computational Linguistics ACL 2024*, pages 8940–8965, Bangkok, Thailand and virtual meeting, August 2024. Association for Computational Linguistics.

Masahiro Kaneko, Danushka Bollegala, and Naoaki Okazaki. The impact of debiasing on the performance of language models in downstream tasks is underestimated. In Jong C. Park, Yuki Arase, Baotian Hu, Wei Lu, Derry Wijaya, Ayu Purwarianti, and Adila Alfa Krisnadhi, editors, *Proceedings of the 13th International Joint Conference on Natural Language Processing and the 3rd Conference of the Asia-Pacific Chapter of the Association for Computational Linguistics (Volume 2: Short Papers)*, pages 29–36, Nusa Dua, Bali, November 2023. Association for Computational Linguistics.

Shahar Katz, Yonatan Belinkov, Mor Geva, and Lior Wolf. Backward lens: Projecting language model gradients into the vocabulary space. *arXiv preprint arXiv:2402.12865*, 2024.

Junsol Kim, James Evans, and Aaron Schein. Linear representations of political perspective emerge in large language models. *arXiv preprint arXiv:2503.02080*, 2025.

Hadas Kotek, Rikker Dockum, and David Sun. Gender bias and stereotypes in large language models. In *Proceedings of The ACM Collective Intelligence Conference*, page 12–24, New York, NY, USA, 2023. Association for Computing Machinery. ISBN 9798400701139.

Samuel Marks, Can Rager, Eric J Michaud, Yonatan Belinkov, David Bau, and Aaron Mueller. Sparse feature circuits: Discovering and editing interpretable causal graphs in language models. In *The Thirteenth International Conference on Learning Representations*, 2025. URL `https://openreview.net/forum?id=I4e82CIDxv`.

Kevin Meng, David Bau, Alex Andonian, and Yonatan Belinkov. Locating and editing factual associations in gpt. *Advances in Neural Information Processing Systems*, 35:17359–17372, 2022.

Neel Nanda, Lawrence Chan, Tom Lieberum, Jess Smith, and Jacob Steinhardt. Progress measures for grokking via mechanistic interpretability. *arXiv preprint arXiv:2301.05217*, 2023.

Pranav Narayanan Venkit, Sanjana Gautam, Ruchi Panchanadikar, Ting-Hao Huang, and Shomir Wilson. Nationality bias in text generation. In Andreas Vlachos and Isabelle Augenstein, editors, *Proceedings of the 17th Conference of the European Chapter of the Association for Computational Linguistics*, pages 116–122, May 2023.

Roberto Navigli, Simone Conia, and Björn Ross. Biases in large language models: Origins, inventory, and discussion. *J. Data and Information Quality*, 15(2), June 2023. ISSN 1936-1955.

Chris Olah. Mechanistic interpretability, variables, and the importance of interpretable bases. transformer circuits thread (june 27), 2022.

Chris Olah, Nick Cammarata, Ludwig Schubert, Gabriel Goh, Michael Petrov, and Shan Carter. Zoom in: An introduction to circuits. *Distill*, 5(3):e00024–001, 2020.

Haoyi Qiu, Zi-Yi Dou, Tianlu Wang, Asli Celikyilmaz, and Nanyun Peng. Gender biases in automatic evaluation metrics for image captioning. In *The 2023 Conference on Empirical Methods in Natural Language Processing*, 2023.

Alec Radford, Jeff Wu, Rewon Child, David Luan, Dario Amodei, and Ilya Sutskever. Language models are unsupervised multitask learners. 2019.

Erik F Sang and Fien De Meulder. Introduction to the conll-2003 shared task: Language-independent named entity recognition. *arXiv preprint cs/0306050*, 2003.

Shweta Soundararajan and Sarah Jane Delany. Investigating gender bias in large language models through text generation. In Mourad Abbas and Abed Alhakim Freihat, editors, *Proceedings of the 7th International Conference on Natural Language and Speech Processing (ICNLSP 2024)*, pages 410–424, Trento, October 2024. Association for Computational Linguistics. URL https://aclanthology.org/2024.icnlsp-1.42/.

Aaquib Syed, Can Rager, and Arthur Conmy. Attribution patching outperforms automated circuit discovery. *arXiv preprint arXiv:2310.10348*, 2023.

Aaquib Syed, Can Rager, and Arthur Conmy. Attribution patching outperforms automated circuit discovery. In Yonatan Belinkov, Najoung Kim, Jaap Jumelet, Hosein Mohebbi, Aaron Mueller, and Hanjie Chen, editors, *Proceedings of the 7th BlackboxNLP Workshop: Analyzing and Interpreting Neural Networks for NLP*, pages 407–416, November 2024.

Hugo Touvron, Louis Martin, Kevin Stone, Peter Albert, Amjad Almahairi, Yasmine Babaei, Nikolay Bashlykov, Soumya Batra, Prajjwal Bhargava, Shruti Bhosale, Dan Bikel, Lukas Blecher, Cristian Canton Ferrer, Moya Chen, Guillem Cucurull, David Esiobu, Jude Fernandes, Jeremy Fu, Wenyin Fu, Brian Fuller, Cynthia Gao, Vedanuj Goswami, Naman Goyal, Anthony Hartshorn, Saghar Hosseini, Rui Hou, Hakan Inan, Marcin Kardas, Viktor Kerkez, Madian Khabsa, Isabel Kloumann, Artem Korenev, Punit Singh Koura, Marie-Anne Lachaux, Thibaut Lavril, Jenya Lee, Diana Liskovich, Yinghai Lu, Yuning Mao, Xavier Martinet, Todor Mihaylov, Pushkar Mishra, Igor Molybog, Yixin Nie, Andrew Poulton, Jeremy Reizenstein, Rashi Rungta, Kalyan Saladi, Alan Schelten, Ruan Silva, Eric Michael Smith, Ranjan Subramanian, Xiaoqing Ellen Tan, Binh Tang, Ross Taylor, Adina Williams, Jian Xiang Kuan, Puxin Xu, Zheng Yan, Iliyan Zarov, Yuchen Zhang, Angela Fan, Melanie Kambadur, Sharan Narang, Aurelien Rodriguez, Robert Stojnic, Sergey Edunov, and Thomas Scialom. Llama 2: Open foundation and fine-tuned chat models, 2023. URL https://arxiv.org/abs/2307.09288.

Jesse Vig, Sebastian Gehrmann, Yonatan Belinkov, Sharon Qian, Daniel Nevo, Yaron Singer, and Stuart Shieber. Investigating gender bias in language models using causal mediation analysis. *Advances in neural information processing systems*, 33:12388–12401, 2020.

Kevin Wang, Alexandre Variengien, Arthur Conmy, Buck Shlegeris, and Jacob Steinhardt. Interpretability in the wild: a circuit for indirect object identification in gpt-2 small. *arXiv preprint arXiv:2211.00593*, 2022.

A Warstadt. Neural network acceptability judgments. *arXiv preprint arXiv:1805.12471*, 2019.

Zhengxuan Wu, Atticus Geiger, Thomas Icard, Christopher Potts, and Noah Goodman. Interpretability at scale: Identifying causal mechanisms in alpaca. In *Thirty-seventh Conference on Neural Information Processing Systems*, 2023. URL https://openreview.net/forum?id=nRfClnMhVX.

Fred Zhang and Neel Nanda. Towards best practices of activation patching in language models: Metrics and methods, 2024. URL https://arxiv.org/abs/2309.16042.

A Description for Biased Dataset

We did an experiment varyting the number of tokens used to computed bias for GPT-2 and Llama-2 and found that beyond 10 tokens the amount of bias present in the model doesn't change that much. Hence we opted for only using 10 tokens to compute bias in LLMs. Table 5 shows the bias computed for each model on different datasets. It also shows the number of instances present in each variation of the dataset along with average length of the input sentences.

B LLMs Explored

We used three different models for our experiments. Each one of them is described as follows.

GPT-2 Small This is a 85M parameter model with 12 layers and 12 attention heads per layer. The model has a dimension of 768 and vocab size of 50257. It uses GELU as its activation function Radford et al. (2019). In its computational graph we have 158 nodes and 32491 edges.

GPT-2 Large This is a larger version of GPT having 708M parameters, with 36 layers and 20 attention heads per layer. This one has a dimension of 1280 and vocab size of 50257. Similar to the smaller version it

Model	Struct Type	Bias Category	#Samples	Length	Bias Metric
GPT-2 Small	DSS1	Positive	92	7.65	0.659
	DSS1	Negative	132	6.72	0.753
	DSS2	Positive	141	9.48	0.637
	DSS2	Negative	83	9.06	0.633
	GSS1	Male	293	11.69	0.816
	GSS1	Female	27	11.74	0.751
	GSS2	Male	291	10.69	0.837
	GSS2	Female	29	10.75	0.787
GPT-2 Large	DSS1	Positive	139	7.65	0.785
	DSS1	Negative	85	6.85	0.742
	DSS2	Positive	69	9.65	0.652
	DSS2	Negative	155	9.18	0.762
	GSS1	Male	290	11.68	0.889
	GSS1	Female	30	11.8	0.823
	GSS2	Male	274	10.66	0.847
	GSS2	Female	46	10.91	0.786
Llama-2	DSS1	Positive	216	7.0	0.853
	DSS1	Negative	8	6.125	0.718
	DSS2	Positive	216	10.0	0.813
	DSS2	Negative	8	9.0	0.665
	GSS1	Male	298	13.33	0.861
	GSS1	Female	22	13.36	0.797
	GSS2	Male	291	13.31	0.864
	GSS2	Female	29	13.55	0.760

Table 5: Dataset Statistics for Different types of Bias Across Different Models. *#Samples*- Number of Samples, *Length*- Avg Length of the sentence. *Bias metric* - Normalized probability of Positive words per example of Postive Bias Category (and similarly the Normalized probability of Negative words per example for Negative Bias Category). Similar strategy for Gender Bias.

uses GELU as its activation function Radford et al. (2019). In its computational graph we have 758 nodes and 810703 edges.

Llama-2 This is a 6.5B parameter model with 32 layers and 32 attention heads per layer. The model has a dimension of 4096 and vocab size of 32000. Unlike GPT-2 versions it employs SiLU as its activation function Touvron et al. (2023). In its computational graph we have 1058 nodes and 1592881 edges.

C Baseline Scoring

We have the option to calculate the baseline scores for both positive-bias and negative-bias datasets via two methods i.e., evaluate-baseline scoring and evaluate-graph scoring. The evaluate-baseline function calculates the difference in probabilities between positive and negative next-token predictions and averages it over the whole dataset. While as in evaluate-graph function we have the option of passing the argument of Graph (A Graph represents a model's computational graph. Once instantiated, it contains various Nodes, representing mostly attention heads and MLPs, and Edges representing connections between nodes. Each Node and Edge is either in the graph (circuit) or not; by default, all Node and Edge objects are included within the graph.), and in the process of calculating the baseline score using evaluate-graph function we need to pass the unaltered graph where no edge or node is ablated yet. Since we are going to use the evaluate-graph function when we ablate some edges, hence it is best to use evaluate-graph function for getting the baseline score which we are going to use to check the importance of edges.

D Finding Bias Circuits

We sort all the edges in the graph according to their scores and print the edges in the descending order with their respective scores for each positive-bias and negative-bias dataset. These scores are the respective edge scores and reveal the importance of the edges in the graph for propagating the respective bias. The more the score, the more important is the edge. The goal here was to ablate the Top N edges in the graph (N ranging from 1 to 10 in our case) and observe the variation in the evaluate-graph scores and compare it to the graph-baseline score. EAP Syed et al. (2023) eventually outputs a sorted list of edges where each edge is represented by the corresponding connecting nodes. In Table 6 we the description of different types of nodes

Node	***Description***	***GPT-2 Small***	***GPT-2 Large***	***Llama-2***
input	Input Node	NA	NA	NA
logits	Logit Node	NA	NA	NA
m{i}	i*th* MLP layer	$i \in (0-11)$	$i \in (0-35)$	$i \in (0-31)$
a{i}.h{j}	j*th* attention head in i*th* attention layer	$i \in (0-11)$, $j \in (0-11)$	$i \in (0-35)$, $j \in (0-19)$	$i \in (0-31)$, $j \in (0-31)$
a{i}.h{j}<x> x=[**q**]uery, [**k**]ey, [**v**]alue	j*th* [x] attention head in i*th* attention layer	$i \in (0-11)$, $j \in (0-11)$	$i \in (0-35)$, $j \in (0-19)$	$i \in (0-31)$, $j \in (0-31)$

Table 6: Nomenclature for Nodes in the computational graph of GPT-2 and Llama-2 (Edges described in Manual Edge Ablation Section in Appendix)

referred in EAP. Thable 7 shows the top 3 edges obtained for different types of bias across different models (i.e. GPT2- Small, GPT2-large and Llama2).

		Top 1		**Top 2**		**Top 3**	
Model	**Bias Type**	**Edge**	**Score**	**Edge**	**Score**	**Edge**	**Score**
GPT-2 Small	Demographic Positive(DSS1)	m11->logits	0.3307	m0->m2	0.1900	m0->m1	0.1858
GPT-2 Small	Demographic Negative(DSS1)	m11->logits	0.2655	m0->m1	0.1684	m0->m2	0.1557
GPT-2 Small	Demographic Positive(DSS2)	m11->logits	0.1580	m0->m2	0.1205	m9->logits	0.0921
GPT-2 Small	Demographic Negative(DSS2)	m11->logits	0.0720	m0->m2	0.0658	m0->m1	0.0527
GPT-2 Large	Demographic Positive(DSS1)	m35->logits	0.3183	m33->m35	0.1732	m33->logits	0.1526
GPT-2 Large	Demographic Negative(DSS1)	m35->logits	0.3219	m33->m35	0.1245	a32.h2->logits	0.1123
GPT-2 Large	Demographic Positive(DSS2)	m35->logits	0.2458	m32->logits	0.1226	m33->m35	0.1070
GPT-2 Large	Demographic Negative(DSS2)	m35->logits	0.1151	m32->logits	0.0598	m0->m4	0.0457
GPT-2 Small	Gender Male(GSS1)	input->m0	0.0663	input->a0.h5⟨k⟩	0.0561	input->a0.h5⟨q⟩	0.0483
GPT-2 Small	Gender Female(GSS1)	input->m0	0.0675	input->a0.h5⟨k⟩	0.0539	m11->logits	0.0471
GPT-2 Small	Gender Male(GSS2)	input->m0	0.0615	input->a0.h5⟨k⟩	0.0602	input->a0.h5⟨q⟩	0.0502
GPT-2 Small	Gender Female(GSS2)	input->m0	0.0649	input->a0.h5⟨k⟩	0.0575	m11->logits	0.0541
GPT-2 Large	Gender Male(GSS1)	m35->logits	0.0281	a33.h11->logits	0.0274	m33->logits	0.0261
GPT-2 Large	Gender Female(GSS1)	m35->logits	0.0206	a33.h11->logits	0.0203	m33->logits	0.0192
GPT-2 Large	Gender Male(GSS2)	m35->logits	0.0306	a33.h11->logits	0.0265	a32.h2->logits	0.0249
GPT-2 Large	Gender Female(GSS2)	m35->logits	0.0241	a32.h2->logits	0.0206	a33.h11->logits	0.0204
Llama-2	Gender Male(GSS1)	m31->logits	0.2467	m30->logits	0.0560	m30->m31	0.0497
Llama-2	Gender Female(GSS1)	m31->logits	0.3141	m30->logits	0.1282	m30->m31	0.0852
Llama-2	Gender Male(GSS2)	m31->logits	0.2618	m30->logits	0.0907	m30->m31	0.0542
Llama-2	Gender Female(GSS2)	m31->logits	0.3308	m30->logits	0.1461	m30->m31	0.1095

Table 7: Top 3 edges for Different Models and Different Bias

E Creating Corrupted Edges for Downstream Tasks

For CoLA dataset we filter the sentence containing atleast one noun, duplicate the sentence and swap every noun token with "XYZ", preserving positions. For CoLA dataset we swap any two randomly chosen words in the sentence.

F SAE Approach Results

SAE Marks et al. (2025) is another recent approach to find important components from a model similar to EAP Syed et al. (2023). In Figure 6, we have done similar experiments like Figure 2 using SAE. Figure 6 shows that there is not much overlap between demographic and gender bias in general.

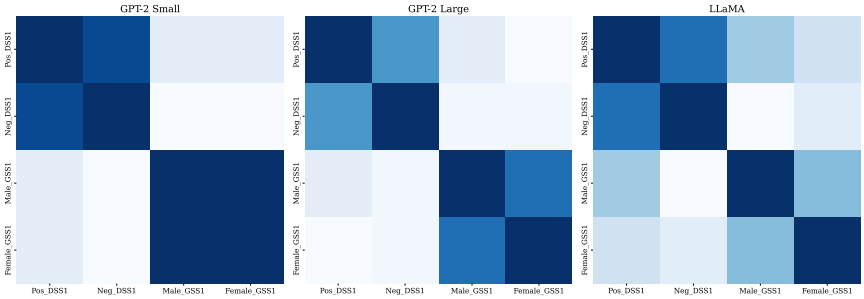

Figure 6: Overlap Results from SAE Approach

G Circuit Diagram

Figure 7 shows the circuit diagram for different types of bias (i.e. demographic and gender) obtained from EAP approach Syed et al. (2023). A circuit is a subgraph of a neural network[3].

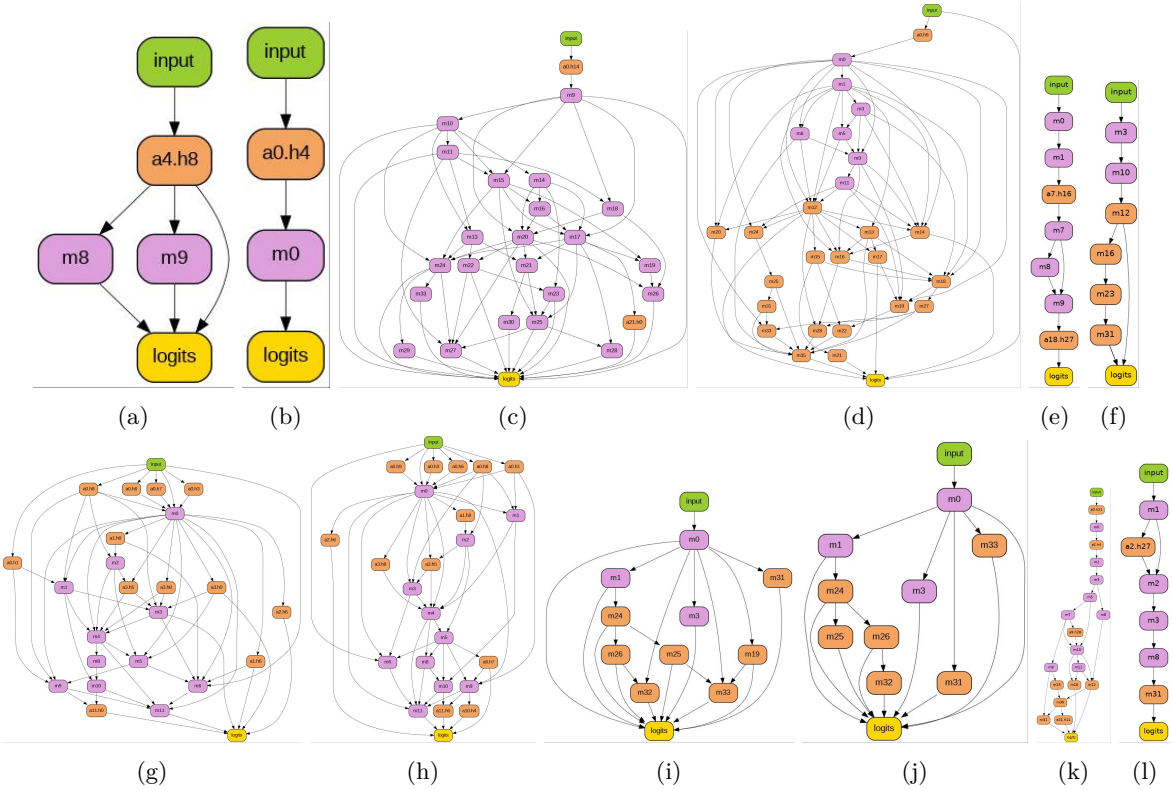

Figure 7: Circuit Diagram: (a) GPT-2-Small-DSS1-Positive, (b) GPT-2-Small-DSS2-Positive, (c) GPT-2-Large-DSS1-Positive, (d) GPT-2-Large-DSS2-Positive, (e) Llama-2-DSS1-Positive, (f) Llama-2-DSS2-Positive, (g) GPT-2-Small-GSS1-Positive, (h) GPT-2-Small-GSS2-Positive, (i) GPT-2-Large-GSS1-Positive, (j) GPT-2-Large-GSS2-Positive, (k) Llama-2-GSS1-Positive, (l) Llama-2-GSS2-Positive.

[3] https://distill.pub/2020/circuits/zoom-in/#glossary-circuit